JOURNAL OF MATERIALS SCIENCE 30 (1995) 1196–1202

Some properties of mullite powders prepared by chemical vapour deposition

Part II *Sinterability*

KIYOSHI ITATANI, TAKAYASU KUBOZONO, F. SCOTT HOWELL, AKIRA KISHIOKA, MAKIO KINOSHITA
Department of Chemistry, Faculty of Science and Engineering, Sophia University, 7-1 Kioi-cho, Chiyoda-ku, Tokyo 102, Japan

The sinterability of mullite ($3Al_2O_3 \cdot 2SiO_2$) powder prepared by chemical vapour deposition was examined to improve the conditions for fabricating dense mullite ceramics. The starting powder contained not only mullite, but also a small amount of γ-Al_2O_3 (Al–Si spinel) and amorphous material. Although the compressed powder was fired at a temperature between 1550 and 1700 °C for 1, 3 and 5 h, the relative densities of the sintered compacts were limited to ~ 90%: (i) due to the creation of pores/microcracks during the solid state reaction (1100–1350 °C), and (ii) due to restriction on the rearrangement of grains because the amount of liquid phase (1550–1700 °C) was insufficient. Calcination of the starting powder was effective for preparation of easily sinterable powder with homogeneous composition. When the compact formed by compressing the calcined powder at 1400 °C for 1 h was fired at 1650 °C for 3 h, the relative density was raised up to 97.2%; moreover, mullite was the only phase detected from the sintered compact. The sintered compact was composed of polyhedral grains with sizes of 1–2 μm and elongated grains with long axes of ~ 6 μm.

1. Introduction

Since mullite ($3Al_2O_3 \cdot 2SiO_2$) ceramics have high thermal resistance [1], low thermal expansion coefficient [2] and high bending strength [3], they should make suitable structural and electronic materials [4, 5]. The dense and high strength mullite ceramics can generally be fabricated from a submicrometre sized mullite powder [5, 6].

Previous ways of sintering submicrometre sized mullite powder can be divided into two types [7, 8]: (i) solid state sintering of crystalline mullite powder, and (ii) viscous sintering of the "premullite" (amorphous or very poorly crystalline) powder. The relative densities of the sintered compacts are 95–99% in both sintering techniques. Although the sintering temperatures (1600–1650 °C) of the crystalline mullite powder are generally higher than those (1200–1250 °C) of the premullite powder, sintering of the crystalline mullite powder has the advantage of forming a more homogeneous microstructure than that produced by sintering of the premullite powder [8].

Powders prepared by chemical vapour deposition (CVD) have been studied. Hori and Kurita [8] prepared premullite powder by flame CVD, and examined the sinterability of this powder; the relative density of the compact fired at 1600 °C for 2 h reached over 98.8%. The present authors have also prepared crystalline mullite by CVD, using electric furnaces [9]; however, little information on the sinterability of this powder is yet available. The purposes of this paper are: (i) to examine the sinterability of mullite powder prepared by the present CVD, and (ii) to determine the optimum sintering conditions for fabricating dense mullite ceramics.

2. Experimental procedure

2.1. Preparation of the starting powder

The mullite powder was prepared by chemical vapour deposition [9], i.e. vapour phase reaction at 1200 °C among aluminium chloride ($AlCl_3$) vapour (sublimation temperature, 180 °C), silicon chloride ($SiCl_4$) vapour (evaporation temperature, 25 °C), and oxygen (O_2). The flow rates of the carrier gas for $AlCl_3$ and for $SiCl_4$ were 0.3 $dm^3 min^{-1}$ and 0.3 $dm^3 min^{-1}$, respectively; the flow rate of O_2 gas was 0.9 $dm^3 min^{-1}$. These gas flow conditions were selected for preparing stoichiometric mullite.

The resulting powder contained not only mullite, but also a small amount of γ-Al_2O_3 and amorphous material [9]. The Al_2O_3 and SiO_2 contents were 72.70 and 27.23%, respectively; these values were almost in accord with those of stoichiometric mullite [9]. Other properties were as follows [9]: specific surface area, 43.5 $m^2 g^{-1}$; primary particle size, 0.046 μm; crystallite size, 0.045 μm; true density, 3.00 $g cm^{-3}$.

2.2. Phase identification

Phase identification of the sintered compact was conducted using an X-ray diffractometer (XRD) with

0022–2461

CuK_{α_1} radiation, operated at 40 kV and 25 mA (Model Rad II A, Rigaku, Tokyo). Electron probe X-ray microanalysis (EPMA; Model EMAX-1000, Horiba, Kyoto) was conducted to examine the distribution states of Al and Si elements in the sintered compact.

2.3. Examination of sinterability

About 0.14 g of the powder was pressed at 300 MPa to form a disc with diameter of 5 mm and thickness of ~ 3 mm; about 0.28 g of the powder was pressed at 100 MPa to form a disc with diameter of 10 mm and thickness of ~ 2 mm. The former was used for dilatometric measurement, whereas the latter was used for measurements of the relative density (bulk density/theoretical density) and for observation of the microstructure of the sintered compact.

The expansion–shrinkage behaviour of the compact was examined from room temperature up to 1700 °C at a heating rate of 10 °C min^{-1} in air, using a dilatometer (Model TMA92, Setaram, Caluire, France). The microstructure of the sintered compact was observed using a scanning electron microscope (SEM; Model S-430, Hitachi, Toyko).

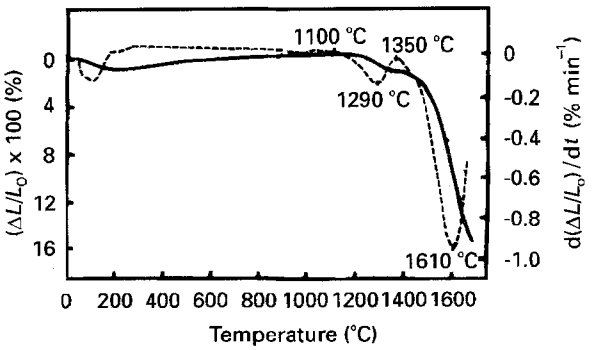

Figure 1 Thermal expansion–shrinkage curve, $\Delta L/L_0$, (——) and its differential curve, $d(\Delta L/L_0)/dt$, (– – –) for compact heated at the rate of 10 °C min^{-1} in air. Note that the starting compact was fabricated by compressing the as-prepared powder.

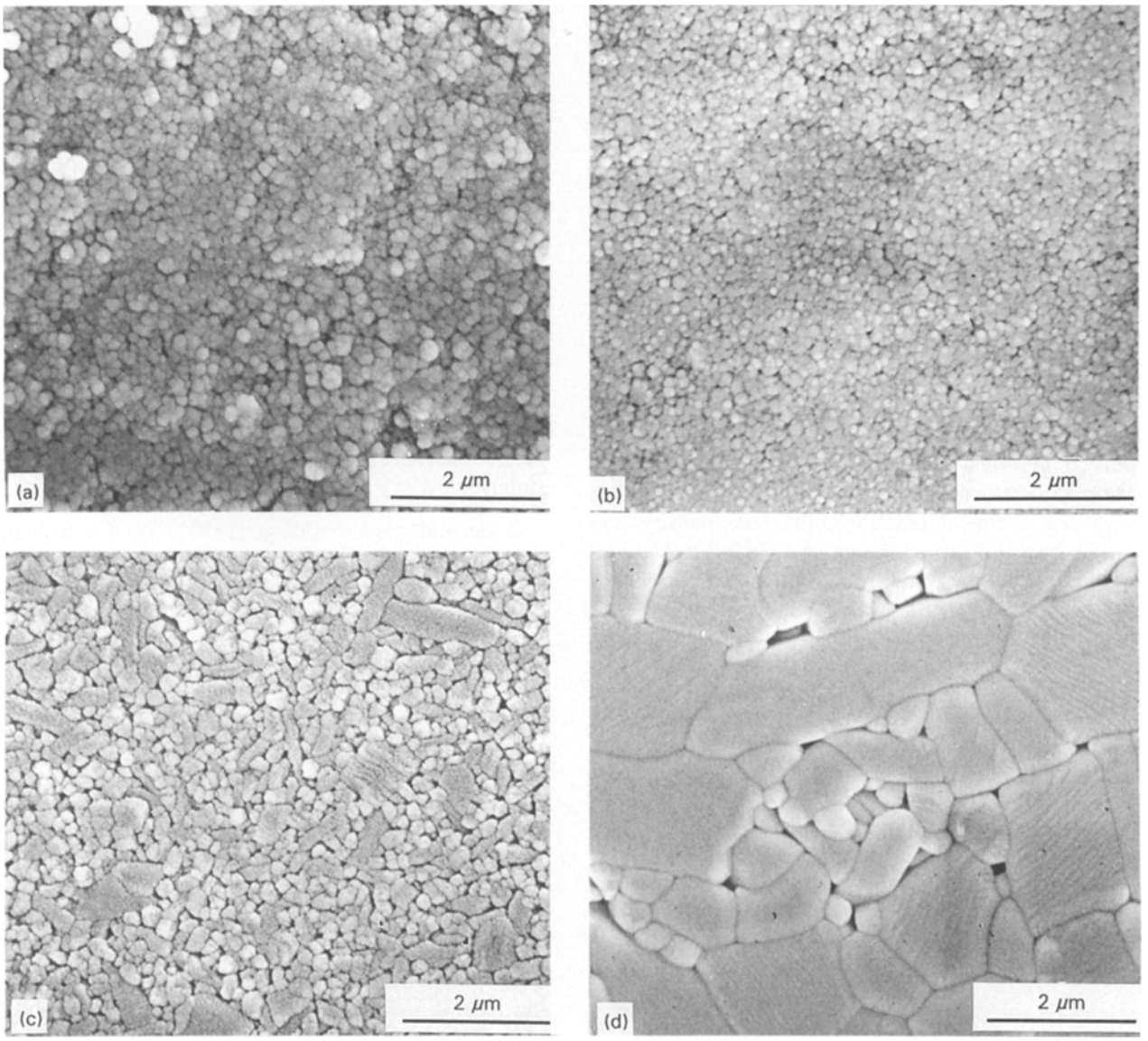

Figure 2 Typical SEM micrographs of the compacts fired at (a) 1100, (b) 1350, (c) 1610 and (d) 1700 °C, respectively. Note that the starting compact was fabricated by compressing the as-prepared powder.

3. Results and discussion

3.1. Properties of as-prepared powder

The densification behaviour and microstructural developments during firing of the compact are reported in this section.

3.1.1. Densification behaviour with increasing temperature

The dilatometric results during the heating of the compact are shown in Fig. 1. Step-wise shrinkage occurred during the heating of the compact, i.e. the first shrinkage step was between 1100 and 1350 °C and the second shrinkage step was between 1350 and 1700 °C. The differential curve showed that the shrinkage rates became maxima at 1290 and 1610 °C.

Since densification of the compact during heating is accompanied by microstructural developments, the microstructures of the compacts heated at various temperatures were observed. Fig. 2 shows typical SEM micrographs of the compacts heated at 1100, 1350, 1610 and 1700 °C. At 1100 °C, Fig. 2a, spherical primary particles/grains with diameters of < 0.5 μm were packed homogeneously. At 1350 °C, Fig. 2b, the microstructure was similar to that at 1100 °C, Fig. 2a, and was composed of spherical primary particles/grains with diameters of < 0.5 μm. At 1610 °C, Fig. 2c, polyhedral grains with sizes of < 0.5 μm and elongated grains with long axes of 1–2 μm were packed closely. At 1700 °C, Fig. 2d, polyhedral grains with sizes of 1–2 μm and elongated grains with long axes of ~ 4 μm were present in the sintered compact.

It has been reported previously [9] that phase changes during heating occur via the following routes: non-stoichiometric mullite (nominal composition; $2Al_2O_3 \cdot SiO_2$) with Al_2O_3-rich composition $\gg \gamma$-Al_2O_3 at room temperature; stoichiometric mullite ($3Al_2O_3 \cdot 2SiO_2$) alone at 1300 °C; stoichiometric mullite $\gg \alpha$-Al_2O_3 at and above 1400 °C. The crystallinity of mullite was enhanced with increasing temperature from room temperature up to 1700 °C. Along with the chemical reactions, the true density was raised from 3.00 to 3.07 g cm^{-3} at 900–1200 °C and from 3.07 to 3.17 g cm^{-3} at 1300–1500 °C; however, little changes in the true density were observed even on further heating [9].

On the basis of these data, the densification behaviour of the present compact can be divided into two stages, i.e. (i) 1100–1350 °C, and (ii) 1350–1700 °C. Each stage is explained below.

1. First stage shrinkage (1100–1350 °C). The compact may shrink in this temperature range because reaction of non-stoichiometric mullite (density, 3.28 g cm^{-3} [10]) with amorphous SiO_2 (2.22 g cm^{-3} [10]) to form stoichiometric mullite [9] results in a reduction of volume

$$3(Al_2O_3 \cdot SiO_2) + SiO_2(\text{amorphous}) \rightarrow 2(3Al_2O_3 \cdot 2SiO_2) \quad (1)$$

Although stoichiometric mullite forms from γ-Al_2O_3 (Al–Si spinel) [9], this reaction causes an expansion, because the density (3.17 g cm^{-3} [11]) of mullite is lower than that (~ 3.67 g cm^{-3} [12]) of γ-Al_2O_3 (Al–Si spinel). Volume reduction due to the increase in density may be confirmed by measuring the true densities of the calcined powders, i.e. 3.05 g cm^{-3} at 1100 °C and ~ 3.10 g cm^{-3} at 1350 °C [9].

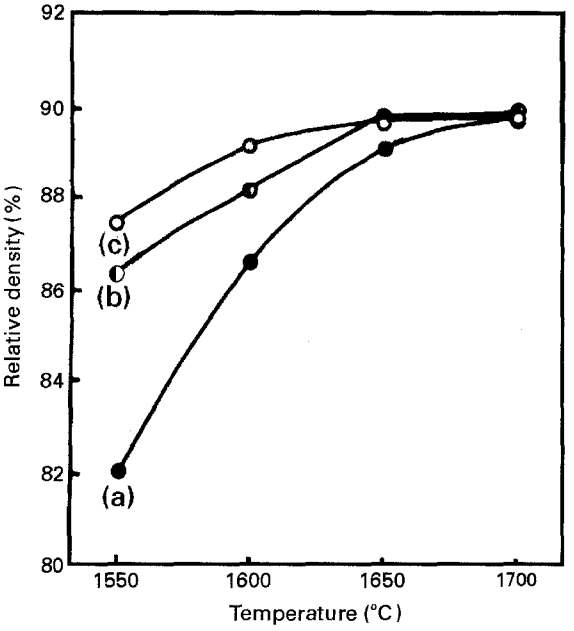

Figure 3 Effect of firing temperature–time on relative density of the sintered compact. Note that the starting compact was fabricated by compressing the as-prepared powder. Firing time: (a) 1, (b) 3, and (c) 5 h, respectively.

Since only tiny changes in primary particle/grain sizes are observed between the compacts heated at 1100 °C, Fig. 2a, and those at 1350 °C, Fig. 2b, it is concluded that the sintering of primary particles does not proceed in this temperature range. Although small pores and/or the microcracks are likely to be created by complex volume reduction [5, 10, 13], they cannot be eliminated easily from the system without any sintering.

2. Second stage shrinkage (1350–1700 °C). Second stage shrinkage may be initiated immediately after the residual non-stoichiometric mullite is decomposed into stoichiometric mullite

$$2(2Al_2O_3 \cdot SiO_2) \rightarrow (3Al_2O_3 \cdot 2SiO_2) + \alpha\text{-}Al_2O_3 \quad (2)$$

Densification starts to occur with the sintering of primary particles or grain growth, which suggests that the pores/microcracks may be eliminated from the system by mass transfer due to solid state sintering of primary particles/grains. Moreover, the elongated grain growth observed at and above 1610 °C, Fig. 2c, d, proves the formation of the liquid phase in the mullite–SiO_2 system [1, 5, 13]; however, the liquid phase formed at the local sites does not promote the rearrangement of grains toward closer packing [14], but promotes elongated grain growth, thus reducing the shrinkage rate at temperatures exceeding 1610 °C.

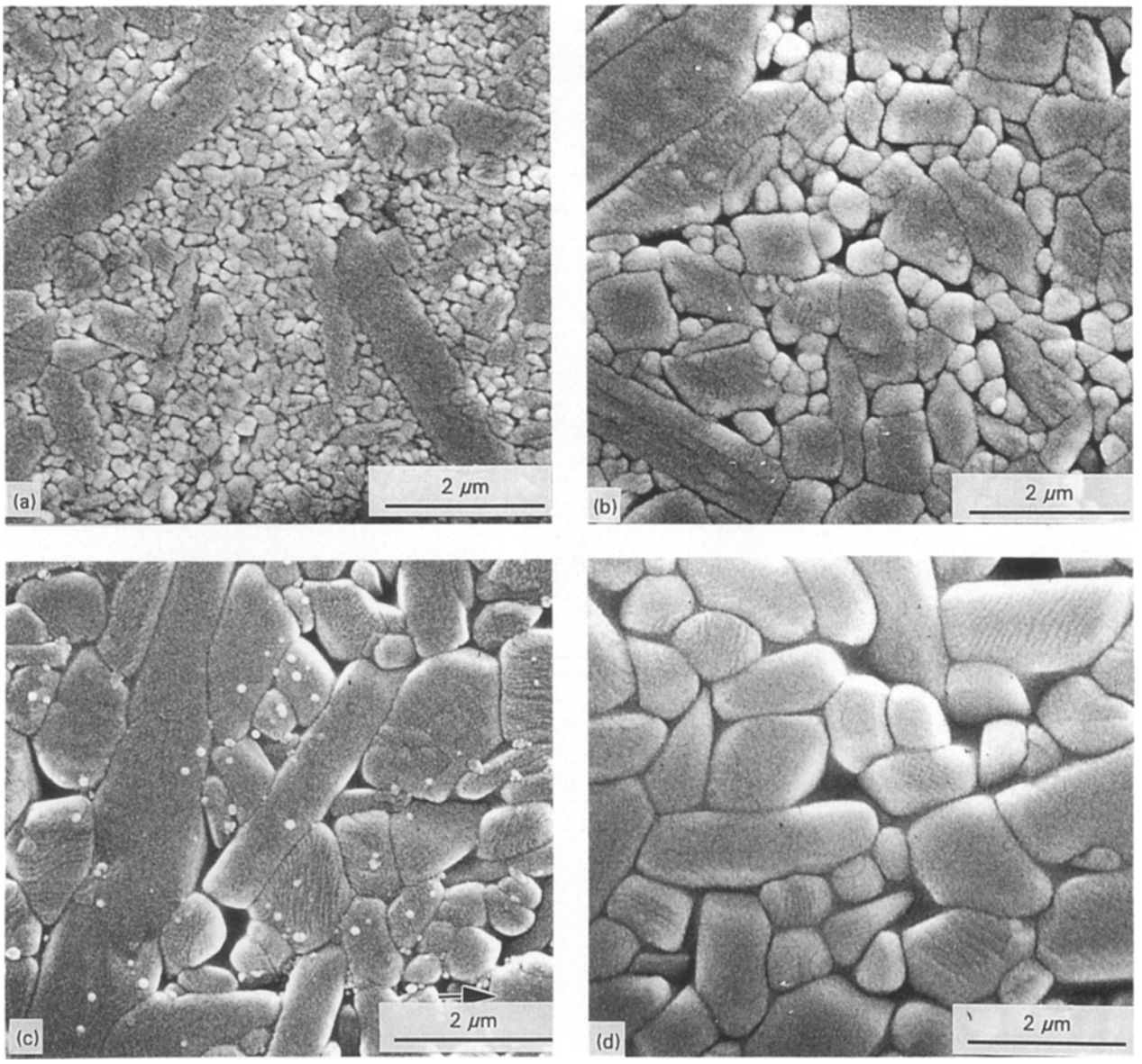

Figure 4 Typical SEM micrographs of the compacts fired at (a) 1550 °C for 5 h, (b) 1600 °C for 5 h, (c) 1650 °C for 5 h and (d) 1700 °C for 5 h. Note that the starting compact was fabricated by compressing the as-prepared powder.

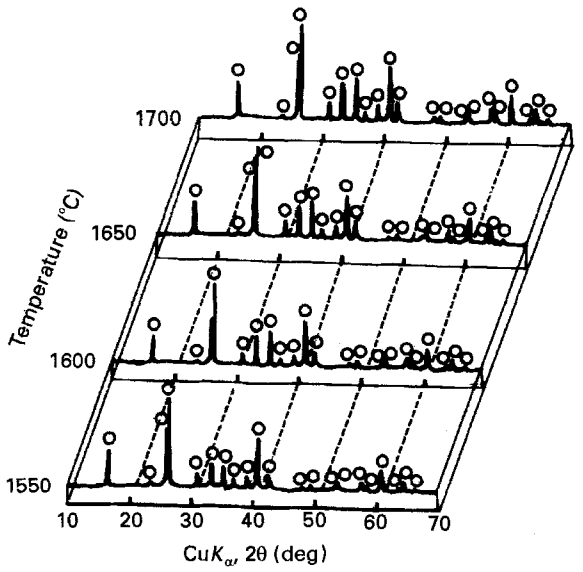

Figure 5 Typical XRD patterns of the compacts fired at various temperatures for 5 h. Note that the starting compact was fabricated by compressing the as-prepared powder: (O) mullite.

3.1.2. Densification behaviour at fixed temperatures

The results in Section 3.1.1. suggest that the firing temperature must be ~ 1600 °C to fabricate dense mullite ceramics. On the basis of this information, the compressed powder is fired at a temperature between 1550 and 1700 °C for 1, 3 and 5 h. Fig. 3 shows the changes in relative density of the sintered compact as functions of firing temperature and time. When the firing time was fixed at 1 h, Fig. 3a, the relative density of the sintered compact increased with increasing temperature and attained 90% at 1700 °C. Although the relative densities of the compacts fired at 1650 °C for 3 h, Fig. 3b and 5 h, Fig. 3c, attained 90%, they were not raised with further increase in firing temperature.

The above results demonstrate that the relative density of the sintered compact attains 90%, but cannot exceed 90%. To make clear the reason why the relative density is limited to 90%, the microstructures of the sintered compacts were first examined using SEM. Typical SEM micrographs are shown in Fig. 4. The

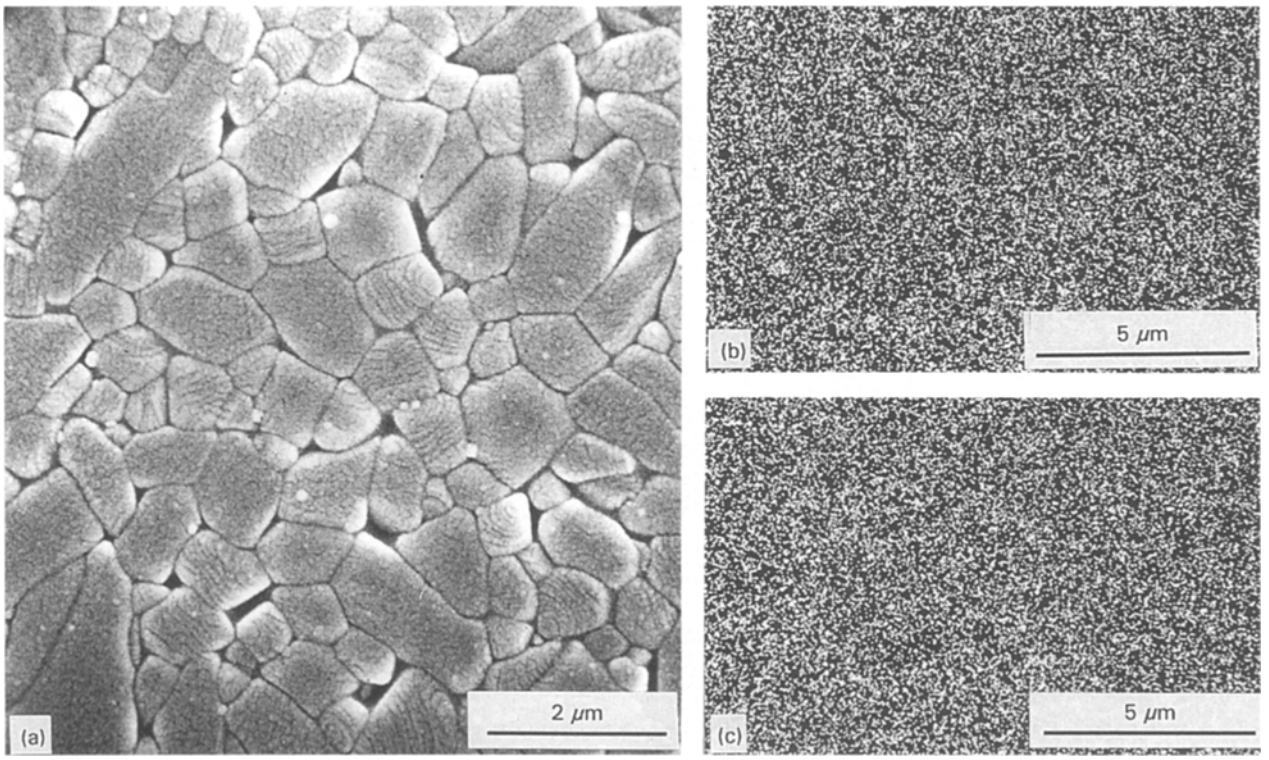

Figure 6 The overall view and EPMA results of the compact fired at 1650 °C for 3 h: (a) overall view, (b) AlK_α and (c) SiK_α.

microstructure of the compact fired at 1550 °C for 5 h, Fig. 4a, showed that elongated grains with long axes of 4–6 μm were present among polyhedral grains with sizes of < 0.5 μm. The microstructure of the compact fired at 1600 °C for 5 h, Fig. 4b, revealed that the polyhedral grains had grown to be 0.5–1 μm; however, the long axis lengths of the elongated grains remained at ~ 6 μm. The microstructure of the compact fired at 1650 °C for 5 h, Fig. 4c, showed that the polyhedral grain sizes grew to be 1–2 μm; the long axes of the elongated grains still remained at ~ 6 μm. The compact fired at 1700 °C for 5 h, Fig. 4d, was composed of polyhedral and rectangular-shaped grains with sizes of 1–6 μm. The overall trend revealed that the growth of polyhedral grains was followed by elongated grain growth and that the pores enlarged with increasing temperature.

The crystalline phases of the above sintered compacts are shown in Fig. 5. These XRD patterns showed that mullite was the only phase detected from the sintered compacts, irrespective of the difference in firing temperature.

The microstructures are composed of two types of grains, i.e. (i) polyhedral grains, and (ii) elongated grains. The polyhedral grains are formed by solid state sintering of the primary particles/grains ($\sim$ 1350–1700 °C), whereas the elongated grains are formed by Ostwald ripening in the presence of the liquid phase of the mullite–SiO_2 system ($\sim$ 1550–1700 °C) [1, 5, 13, 14]. The elongated grains grow faster than the polyhedral grains, because the diffusion rates of Al^{3+} and Si^{4+} through the liquid phase are much faster than those (migration of Al^{3+} into SiO_2 and mullite [15]) through the solid state [14, 16]. The elongation of grains is slowed down with firing temperature, which suggests that the amount of the liquid phase decreases along with "liquid–solid" reaction; consequently, the polyhedral grain sizes approach the rectangular-shaped (former elongated) grain sizes with increasing temperature up to 1700 °C.

The pores/microcracks created by solid state reaction (1100–1350 °C) cannot easily be replaced by solid and/or liquid materials during sintering (1550–1700 °C), because the amount of the liquid phase is too small to rearrange the grains toward closer packing [14]. Thus the fact that the relative density is limited to $\sim 90\%$ may be attributed to (i) the creation of pores/microcracks during solid state reaction (1100–1350 °C), and (ii) restriction on the rearrangement of grains ($\sim$ 1550–1700 °C). Owing to reaction of the liquid phase with the solid material, the composition of the liquid phase shifts toward the mullite-rich side [15]; the "liquid–solid" reaction is not completed until the liquid phase changes into the solid material containing single phase mullite (Fig. 5).

Since grain elongation develops on inhomogeneous microstructure, the firing schedule should be restricted to avoid elongating the grains. A firing temperature and time of 1650 °C and 3 h, respectively were therefore selected. The overall view and EPMA results of the sintered compact are shown in Fig. 6. The sintered compact, Fig. 6a, was composed of polyhedral grains with sizes of 2–4 μm; EPMA results showed that Al, Fig. 6b, and Si, Fig. 6c, were distributed homogeneously.

As the overall view indicates, the grain sizes are more uniform than those of the compact fired at 1650 °C for 5 h, Fig. 4c; moreover, no segregation of the components was observed in the sintered compact, which proves that mullite is the only phase present in the sintered compact.

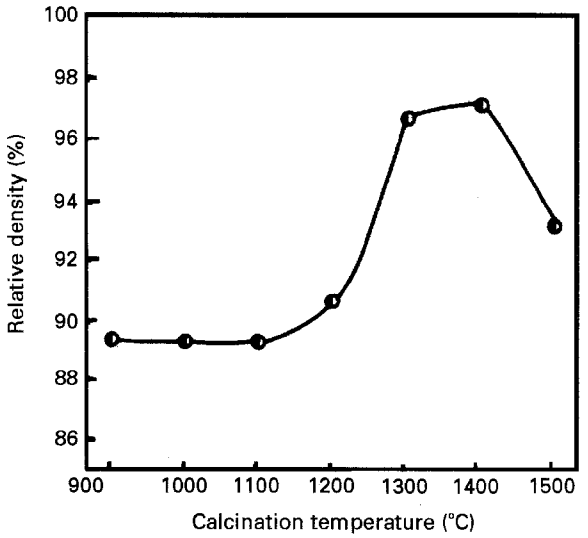

Figure 7 Effect of calcination temperature on relative density of the compact fired at 1650 °C for 3 h: calcination time, 1 h.

3.2. Sinterability of calcined powders

As already described in the previous section, the as-prepared powder contains not only mullite, but also γ-Al_2O_3 (Al–Si spinel) and amorphous material. Since volume reduction due to solid state reactions creates pores/microcracks at 1100–1350 °C [5, 10, 13], one should not try to fabricate a sintered compact with a relative density of over 90%. Thus the as-prepared powder can be calcined at temperatures between 900 and 1500 °C, prior to the sintering operation.

The effect of calcination temperature on the relative density of the compact fired at 1650 °C for 3 h is shown in Fig. 7. In the calcination temperature range of 900–1100 °C, the relative densities of the sintered compacts remained at $\sim$ 89%. The relative density of the sintered compact was raised with a further increase in calcination temperature, and attained 97.2% at 1400 °C; however, the relative density of the sintered

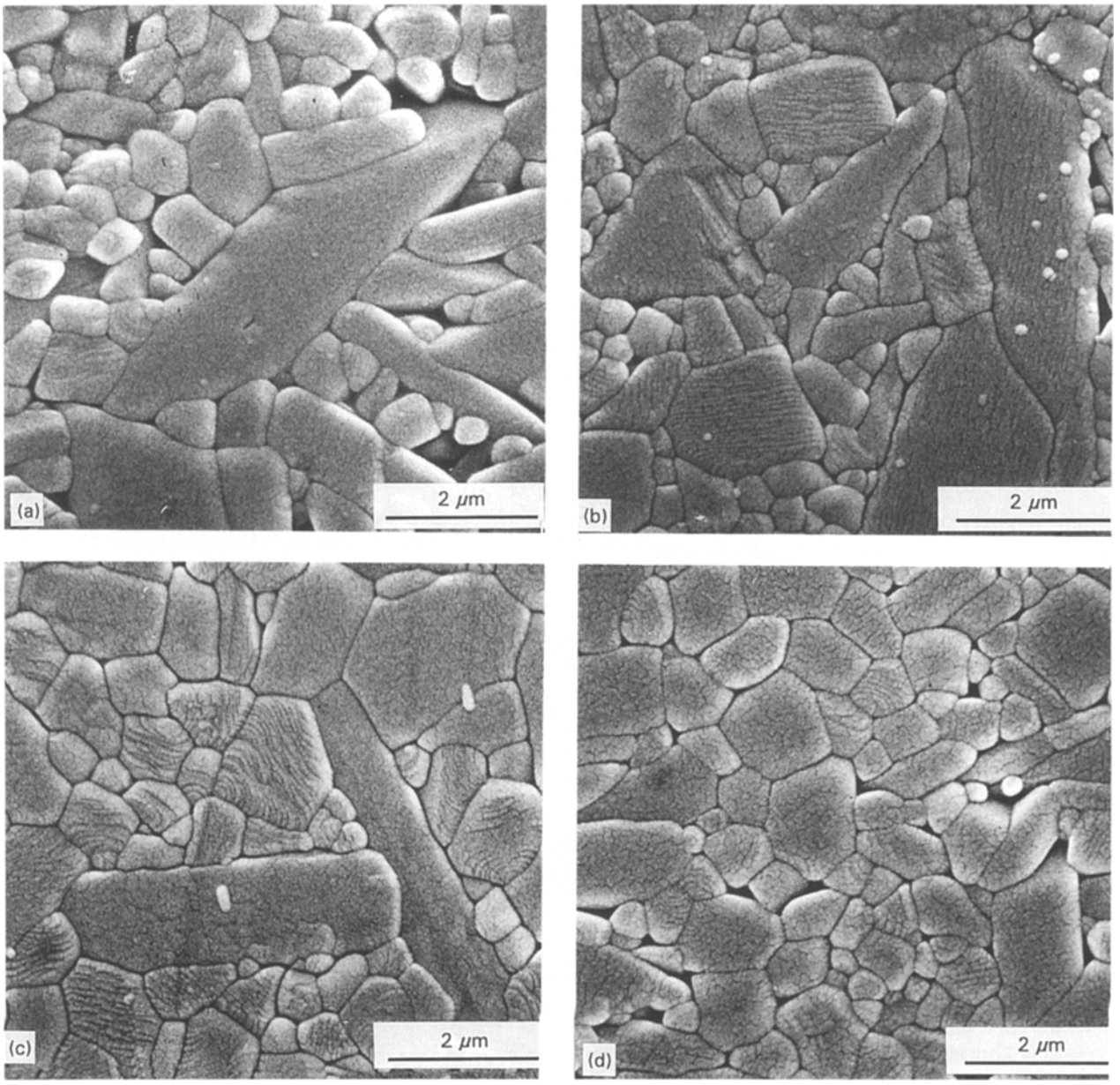

Figure 8 Effect of calcination temperature on microstructure of the compacts fired at 1650 °C for 3 h. Calcination conditions: (a) 900 °C for 1 h, (b) 1200 °C for 1 h, (c) 1400 °C for 1 h, and (d) 1500 °C for 1 h.

compact decreased down to ~ 94% at a calcination temperature of 1500 °C.

Fig. 8 shows typical SEM micrographs of the sintered compacts. At calcination temperatures of 900, 1200 and 1400 °C, Fig. 8a–c, the sintered compacts were composed of polyhedral grains with sizes of 1–2 μm, and elongated grains with long axes of ~ 6 μm; however, the number of elongated grains decreased with increasing calcination temperature. At a calcination temperature of 1500 °C, Fig. 8d, the sintered compact consisted of polyhedral and rectangular-shaped grains with sizes of 1–2 μm; few elongated grains were observed in the sintered compact.

Although the XRD and EPMA data of these sintered compacts were omitted in this paper, mullite was the only phase detected by XRD; moreover, Al and Si elements were homogeneously distributed in the sintered compacts.

The above SEM micrographs indicate that the number of elongated grains decreases with increasing calcination temperature, which suggests that the higher the calcination temperature is, the smaller the amount of liquid phase during the firing becomes. The reason why the relative density of the sintered compact attained 97.2% at a calcination temperature of 1400 °C may be that the formation of pores/microcracks due to the solid state reaction is avoided because most of the solid state reactions are completed during calcination of the as-prepared powder. The relative density of the sintered compact is limited to ~ 94% at a calcination temperature of 1500 °C; this phenomenon may be explained by assuming that the driving force for the sintering is lowered by primary particle growth from 0.01 to 0.02 μm [17]; moreover, the presence of agglomerates due to neck formation of primary particles seems to restrict the final density [18].

As shown in this paper, dense mullite ceramics, with a relative density of 97.2% and with a homogeneous microstructure, can be fabricated using CVD powder; moreover, no milling operation is needed prior to sintering because the starting powder is composed of well dispersed primary particles. Although the present sintering temperature (1650 °C) is higher than that (~ 1300 °C) of the premullite powder [19], the reason may be that interdiffusion rates of Al^{3+} and Si^{4+} in crystalline mullite are low [16], because the present powder is composed of crystalline mullite.

Microstructural investigations to fabricate higher strength mullite ceramics will be continued, because a trace of glassy phase, which tends to remain at the triple points of grains, may reduce the mechanical strength [20, 21].

4. Conclusions

The sinterability of mullite powder prepared by chemical vapour deposition was examined. The results obtained are summarized as follows.

1. The compressed powder was fired at a temperature between 1550 and 1700 °C for 3 h; however, the relative densities of the sintered compacts were limited to ~ 90%, due to the creation of pores/microcracks during solid state reaction (1100–1350 °C) and due to the restricted rearrangement of grains, because the amount of liquid phase (1550–1700 °C) was insufficient.

2. When the compact formed by compressing the powder calcined at 1400 °C for 1 h was fired at 1650 °C for 3 h, the relative density was raised to 97.2%. The sintered compact, with single phase mullite, was composed of polyhedral grains, with sizes of 1–2 μm, and elongated grains, with long axis lengths of ~ 6 μm.

Acknowledgements

The authors express their thanks to Mr K. Maruyama of Rigaku Corp. for the use of the ultra high temperature dilatometer in Setaram, S.A.

References

1. I. A. AKSAY and J. A. PASK, *J. Amer. Ceram. Soc.* **58** (1975) 507.
2. H. SCHNEIDER and E. EBERHARD, *ibid.* **73** (1990) 2073.
3. S. KANZAKI, T. KUMANAGA, J. ASAUMI, O. ABE and H. TABATA, *J. Ceram. Soc. Jpn* **93** (1985) 407.
4. R. R. TUMMALA, *J. Amer. Ceram. Soc.* **74** (1991) 895.
5. I. A. AKSAY, D. M. DABBS and M. SARIKAYA, *ibid.* **74** (1991) 2343.
6. M. D. SACKS, H-W. LEE and J. A. PASK, in "Mullite and Mullite Matrix Composites", edited by S. Sōmiya, R. F. Davis and J. A. Pask (The American Ceramic Society, Westerville, OH, 1990) p. 167.
7. F. KARA and J. A. LITTLE, *J. Mater. Sci.* **28** (1993) 1323.
8. S. HORI and R. KURITA, in "Mullite and Mullite Matrix Composites", edited by S. Sōmiya, R. F. Davis and J. A. Pask (The American Ceramic Society, Westerville, OH, 1990) p. 311.
9. K. ITATANI, T. KUBOZONO, A. KIHIOKA, F. S. HOWELL and M. KINOSHITA, *J. Mater. Sci.* in press.
10. P. D. D. RODRIGO and P. BOCH, *Sci. Ceram.* **13** (1985) C1–405.
11. Powder diffraction file Card No. 15–776 (JCPDS-International Center for Diffraction Data, Swarthmore, PA).
12. Powder diffraction file Card No. 10–425 (JCPDS-International Center for Diffraction Data, Swarthmore, PA).
13. P. D. D. RODRIGO and P. BOCH, *Int. J. High Technol. Ceram.* **1** (1985) 3.
14. A. M. GERMAN, "Liquid Phase Sintering" (Plenum Press, New York, 1985) p. 1.
15. R. F. DAVIS and J. A. PASK, *J. Amer. Ceram. Soc.* **55** (1972) 525.
16. N. SHINOHARA, D. M. DABBS and I. A. AKSAY, *Proc. SPIE-Int. Soc. Opt. Eng.* **683** (1986) 19.
17. K. ITATANI, A. ITOH, F. S. HOWELL, A. KISHIOKA and M. KINOSHITA, *J. Mater. Sci.* **28** (1993) 719.
18. M. O. SACKS and J. A. PASK, *J. Amer. Ceram. Soc.* **65** (1977) 70.
19. W. G. FAHRENHOLZ, D. M. SMITH and J. CESARANO III, *ibid.* **76** (1993) 433.
20. J. S. LEE and S. C. YU, *J. Mater. Sci.* **27** (1992) 5203.
21. H. OHNISHI, T. KAWANAMI, A. NAKAHIRA and K. NIIHARA, *J. Ceram. Soc. Jpn* **98** (1990) 541.

Received 3 February
and accepted 29 June 1994